Calculation of a surface-induced polar effect in nematic liquid crystals

Jinhyoung Lee, Seong-Woo Suh, Kyehun Lee, and Sin-Doo Lee
Physics Department, Sogang University, C.P.O. Box 1142, Seoul 100-611, Korea
(Received 6 August 1993)

We report accurate numerical results for a surface-induced polar effect in a nematic liquid crystal, associated with the symmetry breaking of anisotropic interfacial interactions. By performing numerical simulations, the orientational profiles of the director, the surface molecular tilt, and the resulting optical phase shift are obtained as a function of both the anchoring strength and an external electric field E. In a simple geometry with homogeneous boundary conditions, the polar effect is directly related to the difference in the anchoring energy, and its magnitude depends primarily on E^{-2}.

PACS number(s): 61.30.Gd, 78.20.Jq

The interaction between a liquid crystal (LC) and a treated substrate is important for a basic understanding of physical phenomena at an interface as well as for practical applications. For instance, the broken symmetry and specific interactions at an interface lead, under various circumstances, to novel orientational phenomena [1,2] in the layer adjacent to the interface which may not be observable in the bulk. Moreover, the control of molecular orientation and surface tilt play a critical role in many electro-optic devices.

It is known that a properly treated solid substrate can preferentially orient the constituent molecules of LC's in a certain direction, as a result of anisotropic interfacial interactions between the molecules and the substrate [3]. Particularly, considerable interest has been focused on the interfacial properties of the nematic phase [4] which is characterized by only the presence of orientational order. Due to the inversion symmetry, most of the couplings of this system with external fields are quadratic in nature, as for example, the coupling of the dielectric anisotropy with an external electric field. However, a coupling of the induced polarization associated with the orientational distortions can produce a linear effect which is known as the flexoelectric effect [5].

Recently, it has been demonstrated [6,7] that a strong polar effect, having the flexoelectric origin, exists in a planar sample with two different polymer layers. Typical homogeneous samples exhibit no polar effect but only surface domains [8] are observed. In this Brief Report we perform accurate calculations of the external symmetry-breaking effect of the interfacial interactions between two surface layers on the polar electro-optic properties of LC's. The resultant polar effect is discussed in terms of physical parameters such as surface tilts and anchoring strengths. It is found that the optical phase difference depends primarily on E^{-2} of the applied electric field.

For symmetrical interfaces, in the presence of an external electric field above the Fréedericksz threshold [9], two flexoelectrically induced polarizations in the upper and lower regions of the sample exactly cancel, while for asymmetrical interfaces, a net polarization exists and couples with the electric field to produce the polar effect. This suggests that asymmetry in the interfacial interactions is an essential factor for realizing the polar effect. Experimentally, we confirmed the existence of this polar effect in a commercial material $E7$ (from EM Chemicals) at room temperature [6,7]. Two different interfaces were produced by using two different aligning polymers, poly(1,4-butylene terephthalate) (PBT), which contains aromatic rings which resemble the cores of the liquid-crystal molecules, and nylon 6,6 (NYL), which resembles the tails of the liquid-crystal molecules [10]. It should be noted that no polar effect was observed for the sample made up with the same polymer layers on both surfaces.

In order to examine the polar effect more accurately, we perform numerical simulations for the bulk orientational distortions, the surface tilts, and the optical phase difference as a function of the anchoring energy, the electric field, and material parameters such as the magnitude of the flexoelectric coefficient and the dielectric anisotropy. We use two different methods; one is based on a direct integration of the Euler-Lagrange equation that minimizes the free-energy density and the other uses the relaxation method applicable to solve a full dynamical problem. In the first case, the director orientation and its rate of change in space is estimated at one of two surfaces. The differential equation is then numerically integrated to the other surface through the bulk. When the integration does not yield a desired orientation at the surface, the initial conditions are varied, with the restrictions imposed by the problem, until it does. In the second, an initial configuration is assigned to the director orientation and adjusted to satisfy the equation of motion which causes the free energy to relax toward a minimum [11]. Although this method is more general, it takes long time to obtain the correct equilibrium configuration. Here, we are concerned with only a static problem by using this relaxation method. Once the director configuration is found, the optical-path difference can be computed by using a 2×2 Jones matrix method [12].

For numerical simulations by the first method described above, we construct a usual free energy of a nematic sample of thickness d, aligned homogeneously along the y axis, in the presence of an electric field $\vec{E}$ in the z direction. Assume that the dielectric anisotropy ϵ_a is positive and the distortions, mostly splay, occur along the z direction. Denoting partial derivatives by

subscripts, the free-energy density f per unit area can be written as

$$f = \int_0^d dz[(K_1/2)(1 + \kappa \sin^2\theta)\theta_z^2 - \bar{e}E\sin\theta\cos(\theta)\theta_z - (1/8\pi)\epsilon_a E^2 \sin^2\theta] + f_{\rm sur}, \quad (1)$$

where $\bar{e}$, K_1, and K_3 represent the mean flexoelectric coefficient, the splay elastic constant, and the bend elastic constant, respectively. The anisotropy in the elastic constant is denoted by $\kappa = (K_3 - K_1)/K_1$. Here $f_{\rm sur}$ denotes the surface anchoring energy, and the space-charge effects were ignored. Minimizing the free energy, Eq. (1), the Euler-Lagrange equation leads to

$$(1 + \kappa \sin^2\theta)\theta_{zz} + \kappa \sin\theta\cos(\theta)\theta_z^2 + \xi^{-2}\sin\theta\cos\theta = 0 \quad (0 < z < d), \quad (2)$$

where the dielectric coherence length ξ is given by $\sqrt{4\pi K_1/\epsilon_a E^2}$. The boundary condition represents the torque balance at each surface:

$$(\partial f/\partial\theta_z) \pm (\partial f_{\rm sur}/\partial\theta) = 0 \quad (3)$$

at $z = 0$ and $z = d$, respectively. Macroscopically, the effect of the surface torque can be described in terms of an anisotropic interfacial energy which depends on both the surface tilt and the anchoring strength. For simplicity, we choose the interfacial energy $f_{\rm sur}$ in a form [13] $W(\hat{s}\cdot\vec{n})^2 = W\sin^2\theta$ with the surface normal $\hat{s}$ and the director $\vec{n}$, ignoring terms of surface polarization ($\propto \sin\theta$) on homogeneous surfaces [14]. Accordingly, the two boundary conditions can be rewritten as

$$K_1(1 + \kappa\sin^2\theta_{1,2})\theta_z|_{1,2} - \bar{e}E\sin\theta_{1,2}\cos\theta_{1,2} \pm W_{1,2}\sin\theta_{1,2}\cos\theta_{1,2} = 0. \quad (4)$$

We first obtain the results in the one constant approximation ($\kappa = 0$), and discuss the effect of the anisotropy κ on the optical phase difference associated with the polar effect later. The integration of the Euler-Lagrange equation yields $z = \xi\int^{\theta}(C - \sin^2\alpha)^{-1/2}d\alpha$, where C is a field-dependent integration constant which can be determined from the boundary conditions, Eq. (4). Although numerical calculations are required to exactly solve the equation for $z(\theta)$, it is interesting to see the qualitative features of the infinitely anchored case ($W_{1,2} \to \infty$). Near the Fréedericksz threshold E_c, the maximum distortion angle $\theta_m \propto (E/E_c - 1)^{1/2}$, which is a characteristic of the second-order transition, and $\theta(z) \approx \theta_m \sin(\pi z/d)$. The optical-path difference $\delta \approx n_e d\nu(E/E_c - 1)$ where $\nu = [(n_e/n_o)^2 - 1] \ll 1$ with n_e and n_o the extraordinary and ordinary refractive indices, respectively. For sufficiently high fields, a complete distortion of the sample is obtained, and the maximum distortion angle θ_m becomes $\pi/2$.

Based on Eqs. (2) and (4), together with the literature values of $K = (1/2)(K_1 + K_3) = 1.57 \times 10^{-7}$ dyn in one constant approximation, $\epsilon_a = 13.8$, $\bar{e} = 8 \times 10^{-4}$ cgs unit for the $E7$ material [15,16], $W_1 = 0.10$ dyn/cm, $W_2 = 0.10$ or 0.15 dyn/cm, we carried out accurate calculations to evaluate the orientational distortions $\theta(z)$ for the symmetrical and asymmetrical cases as a function of z/d for fixed electric field E. Figures 1(a) and 1(b) show the numerical results for the two cases, respectively. As expected, for the symmetrical case, the differences in $\theta(z)$ between $(+)E$ and $(-)E$ are identical and symmetric with respect to $z/d = 0.5$. However, for the asymmetrical case, the difference in $\theta(z)$ at the weakly anchored surface is larger than at the strongly anchored one. This difference directly results in the optical-path difference. We confirmed that the two methods employed produce identical results within less than 1% error.

In Figs. 2(a) and 2(b), the surface tilts, θ_1 and θ_2, are plotted as a function of the anchoring energy, W_1, varied

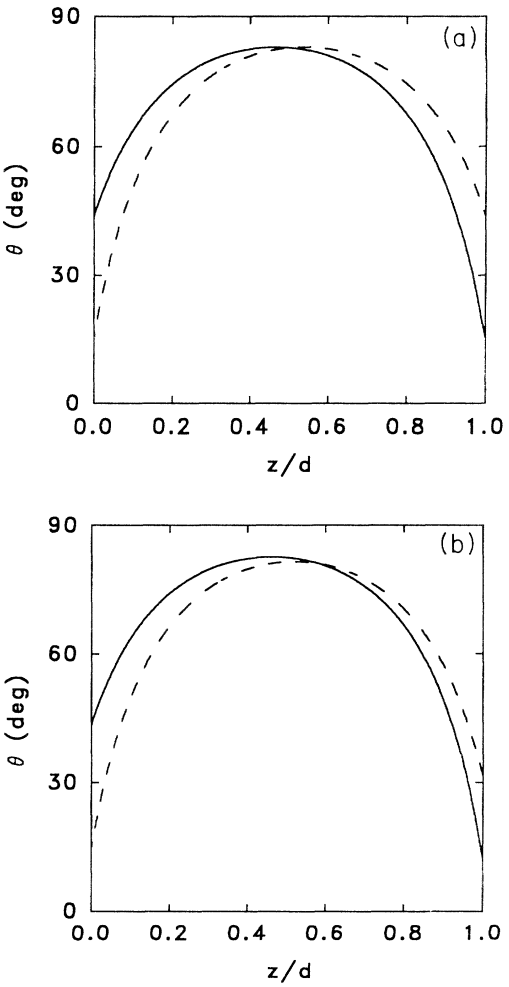

FIG. 1. The spatial distortion angle θ as a function of the normalized z/d for (a) the symmetrical surfaces with the anchoring energies $W_1 = W_2 = 0.10$ dyn/cm, and (b) asymmetrical surfaces with the anchoring energies $W_1 = 0.10$ dyn/cm and $W_2 = 0.15$ dyn/cm, respectively. The electric field $E = 2.5$ V/μm, the dielectric anisotropy $\epsilon_a = 13.8$, and the flexoelectric coefficient $\bar{e} = 8 \times 10^{-4}$ cgs unit. The solid and dashed lines represent two polarities of the electric field $(\pm)E$, respectively.

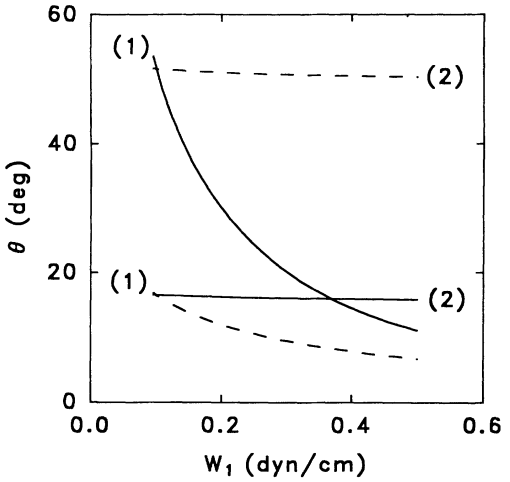

FIG. 2. The surface tilt θ at the two surfaces, (1) and (2), with anchoring energies W_2 fixed as 0.15 dyn/cm and W_1 varied, respectively. The electric field $E = 3.0$ V/μm. The solid and dashed lines represent two polarities of the electric field $(\pm)E$, respectively.

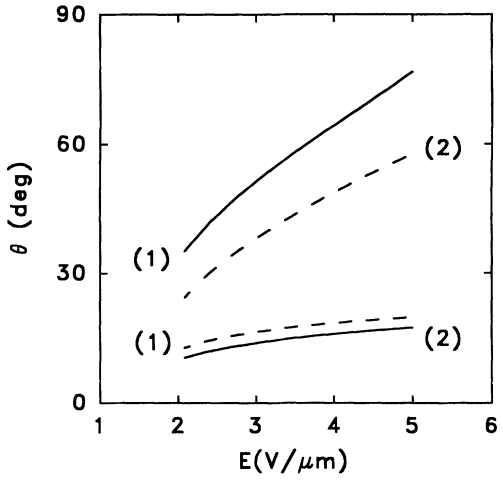

FIG. 3. The surface tilt θ at the two surfaces, (1) and (2), with anchoring energies $W_1 = 0.10$ dyn/cm and $W_2 = 0.15$ dyn/cm, respectively, as a function of the electric field E. The solid and dashed lines represent two polarities of the electric field $(\pm)E$, respectively.

at one surface, and $W_2 = 0.15$ dyn/cm, fixed at the other. It is clearly seen that for a given field E, the surface tilt and its difference between $(+)E$ and $(-)E$ become larger with decreasing anchoring energy. Furthermore, the surface tilt is inversely proportional to the anchoring energy. Qualitatively, this behavior can be understood as follows. Suppose that the sample cell consists of two surface layers where the angle $\theta(z)$ varies continuously from $\theta_m \approx \pi/2$ to θ_1 and θ_2, respectively. For surface tilts up to quadratic order, the first integral of Eq. (2) which satisfies $\theta \approx \pi/2$ and $\theta_z \approx 0$ near the middle of the sample, and Eq. (4) yield the field dependence of θ_1 and θ_2.

$$\theta_{1,2}(E) \approx [(\xi/\eta \pm \xi/b_{1,2})^2 + 1]^{-1/2}, \tag{5}$$

where the flexoelectric coherence length $\eta = K/\bar{e}E$ and the extrapolation length $b_{1,2} = K/W_{1,2}$. The flexoelectric coupling tends to amplify the surface tilt on one surface and to reduce that on the other, which will be clearly shown from numerical results. As $b_{1,2} \to 0$, then $\theta_1 \approx \theta_2 \to 0$, which is the case of the infinite anchoring.

Figures 3(a) and 3(b) show the surface tilts, θ_1 and θ_2, as a function of the electric field E for $W_1 = 0.10$ dyn/cm and $W_2 = 0.15$ dyn/cm. The surface tilt monotonically increases with increasing E. The relative difference in the surface tilts between $(+)E$ and $(-)E$ is proportional to that in the anchoring energies.

We now calculate the optical-path difference δ due to the deformations under consideration:

$$\delta = n_e \left(d - \int_0^d [1 + \nu \sin^2\theta(z)]^{-1/2} dz \right). \tag{6}$$

The resulting polarity-dependent path difference $\Delta\delta$ is then given by

$$\Delta\delta = [\delta(+E) - \delta(-E)]/2. \tag{7}$$

If the two interfaces are identical, then $\Delta\delta = 0$, independent of the polarity of the field E. With the help of the accurate solution of $\theta(z)$ to Eq. (2) with proper boundary conditions, Eq. (4), the optical-path difference $\Delta\delta$ can be obtained. The path difference computed by using the 2×2 Jones matrix method is in excellent agreement with those obtained by Eq. (7).

Figure 4 shows the phase shift, $\Phi = 2\pi\Delta\delta/\lambda$, of the ac

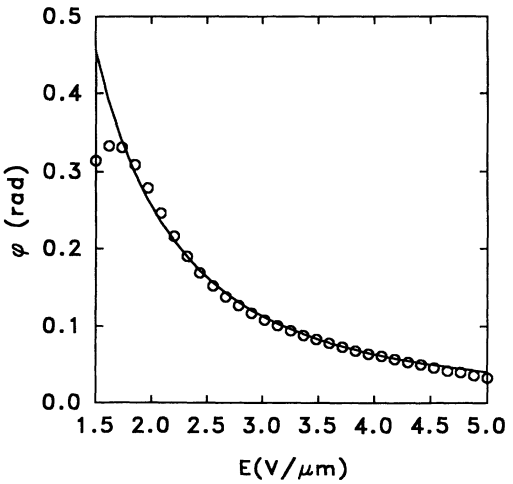

FIG. 4. The optical phase shift Φ due to the polar effect as a function of the applied field E. The material parameters being used are $W_1 = 0.10$ dyn/cm, $W_2 = 0.15$ dyn/cm, the dielectric anisotropy $\epsilon_a = 13.8$, and the flexoelectric coefficient $\bar{e} = 8 \times 10^{-4}$ cgs unit. The solid line was fitted to a form of $\Phi_b + \sum_n a_n/E^n$ $(n \leq 3)$ with $\Phi_b \approx 0$.

transmitted intensity, where $\lambda = 0.514$ μm, $n_o = 1.522$, and $\Delta n = 0.224$ are used [15,16]. The phase shift was fitted to a form of $\Phi_b + \sum_n a_n/E^n$ $(n \leq 3)$ where Φ_b represents a background phase shift ($\Phi_b \approx 0$) and a_n's denote constants that depend on such material parameters as n_e, n_o, $\bar{e}$, K, and the interfacial energy difference (ΔW). Note that the difference ΔW used for numerical simulations is 5.0×10^{-2} dyn/cm which is comparable to the strength for weak anchoring. The fitted values of a_n's are $a_1 \approx 0$, $a_2 = 1.012$, and $a_3 = 0.014$, respectively. This tells us that the phase shift decays predominantly as E^{-2}, which agrees well with the previous results [6]. Also, the same order of the magnitude of a_2 was found. One interesting feature is that the E^{-2} dependence becomes profound [17] with decreasing the magnitude of ϵ_a. For the case of $\kappa \neq 0$, taking $K_1 = 1.08 \times 10^{-7}$ dyn and $K_3 = 2.05 \times 10^{-7}$ dyn [16], it was found that the resulant phase shift is quite insensitive to κ (at most 9% difference) for a given field. This is physically reasonable since mostly splay deformations are involved in our case.

Another point is that the phase shift becomes smaller at higher frequencies. In fact, the thickness ξ of the surface layers will increase with decreasing the field strength E. Since the elastic distortion of a surface layer will relax like $(\gamma/K)\xi^2$ (with γ the relevant viscosity) [18], a full response at frequencies f above $f_c \approx K/(\gamma\xi^2) \approx \epsilon_a E^2/\gamma$ is not expected. Thus, the $1/f$ divergence of the maximum response should terminate at $f \approx K/(\gamma d^2)$, which is the frequency corresponding to the relaxation of a surface layer of thickness equal to the sample thickness d. Further simulations on the frequency dependence by the relaxation method would provide useful information about the dynamics of the surface states.

In summary, we have presented accurate numerical results for a strong polar effect in a homogeneously aligned nematic liquid crystal, associated with the asymmetry in the anisotropic interfacial interactions between two surface layers. We have employed two simulation methods, one of which is a powerful tool for solving a full dynamical problem. The resulting optical phase shift decays essentially as E^{-2}, which is in good agreement with the experimental results [6]. This E^{-2} dependence becomes profound as the dielectric coupling decreases. The difference ΔW required for realizing this polar effect is of the order of 1.0×10^{-2} dyn/cm. The complete picture of its dynamical behavior would be useful for describing other surface phenomena associated with the symmetry breaking, imposed externally.

This work was supported in part by KOSEF through Project No. 93-48-00-02 and SRC.

[1] W. Chen, M. B. Feller, and Y. R. Shen, Phys. Rev. Lett. **63**, 2665 (1989); W. Chen, L. J. Martinez-Miranda, H. Hsiung, and Y. R. Shen, *ibid.* **62**, 1860 (1989).
[2] P. Guyot-Sionnest, H. Hsiung, and Y. R. Shen, Phys. Rev. Lett. **57**, 2963 (1986).
[3] For a comprehensive discussion, see J. Cognard, *Alignment of Nematic Liquid Crystals and Their Mixtures* (Gordon and Breach, London, 1982).
[4] T. J. Sluckin and A. Poniewierski, in *Fluid Interfacial Phenomena*, edited by C. A. Croxon (Wiley, New York, 1986), Chap. 5, and references therein.
[5] R. B. Meyer, Phys. Rev. Lett. **22**, 918 (1969).
[6] S.-D. Lee and J. S. Patel, Phys. Rev. Lett. **65**, 56 (1990).
[7] S.-D. Lee and J. S. Patel, Mod. Phys. Lett. B **4**, 1071 (1990).
[8] H. P. Hinov, Mol. Cryst. Liq. Cryst. **89**, 227 (1982).
[9] See, for example, P. G. de Gennes, *The Physics of Liquid Crystals* (Clarendon Press, Oxford, 1974).
[10] J. S. Patel, T. M. Leslie, and J. W. Goodby, Ferroelectrics **59**, 129 (1984); J. M. Geary, J. W. Goodby, A. R. Kmetz, and J. S. Patel, J. Appl. Phys. **62**, 4100 (1987).
[11] W. H. Press, B. P. Flannery, S. A. Teukolsky, and W. T. Vetterling, *Numerical Recipes* (Cambridge, New York, 1986).
[12] A. Lien, Appl. Phys. Lett. **57**, 2767 (1990); K. Lu and B. E. A. Saleh, Opt. Lett. **17**, 1557 (1992).
[13] A. Rapini and M. Papoular, J. Phys. Colloq. (Paris), **30**, C4-54 (1969).
[14] A. Derzhanski, A. G. Petrov, and M. D. Mitov, J. Phys. (Paris) **39**, 273 (1978).
[15] D. W. Berreman, in *The Physics and Chemistry of Liquid Crystal Devices*, edited by G. J. Sprokel (Plenum Press, New York, 1980), Chap. 1.
[16] M. Schadt and F. Müller, IEEE Trans. Electron Devices **ED-25**, 1125 (1978).
[17] J. Lee, S.-W. Suh, and S.-D. Lee (unpublished).
[18] S.-D. Lee, B. K. Rhee, and Y. J. Jeon, J. Appl. Phys. **73**, 480 (1993).